Synthesis of Chemical Species Relevant in Environmental and Astro Chemistry: Their Production and Characterization by Synchrotron Radiation

Marco Parriani[1,2], Eleonora Manuali[1], Simonetta Cavalli[2], Michele Alagia[3], Robert Richter[4], Stefano Stranges[5,3], Raimund Feifel[6], and Stefano Falcinelli[1(✉)]

[1] Department of Civil and Environmental Engineering, University of Perugia, Via G. Duranti 93, 06125 Perugia, Italy
stefano.falcinelli@unipg.it
[2] Department of Chemistry, Biology and Biotechnologies, University of Perugia, Via Elce di Sotto 8, 06100 Perugia, Italy
simonetta.cavalli@unipg.it
[3] IOM CNR Laboratorio TASC, 34012 Trieste, Italy
alagia@iom.cnr.it
[4] Sincrotrone Trieste, Area Science Park, 34149 Basovizza, Trieste, Italy
robert.richter@elettra.trieste.it
[5] Department of Chemistry and Drug Technology, University of Rome Sapienza, 00185 Rome, Italy
stefano.stranges@uniroma1.it
[6] Department of Physics, University of Gothenburg, Origovägen 6B, 412 58 Gothenburg, Sweden
raimund.feifel@physics.gu.se

Abstract. In this work, the synthesis performed for neutral precursors (isothiocyanic acid, carbon suboxide and cyanoacetylene) used in studies of double photoionization spectroscopy with synchrotron radiation are presented. They were performed starting from few data present in the literature by modifying the procedure in order to obtain a better yield of the desired product with an optimized timing. All the synthetic procedures are related to chemical species of great relevance from an environmental and astrochemical point of view and not commercially available. They can be easily reproduced by any researcher interested in studying the chemical species that are the subject of this work.

Keywords: Astrochemistry · Double Photoionization · Synchrotron Radiation

1 Introduction

1.1 The Photoionization

A general property in thermodynamics is that all objects tend to seek the minimum energy state with the maximum entropy. Similarly, electrons in atoms and molecules, unless influenced by an external force, are found in an energetic local minimum known as

© The Author(s), under exclusive license to Springer Nature Switzerland AG 2026
O. Gervasi et al. (Eds.): ICCSA 2025 Workshops, LNCS 15888, pp. 300–314, 2026.
https://doi.org/10.1007/978-3-031-97596-7_20

the ground state. According to the Aufbau principle, electrons fill lower-energy orbitals before occupying higher-energy ones. Photoionization studies here discussed investigate processes initiated in ground state molecules when they are exposed to photons in the ultraviolet and X-ray spectral regions using tunable synchrotron radiation. The absorbed photon energy may ionize the molecule by ejecting one or more electrons, causing single or multiple ionization. The resulting ion naturally seeks to minimize its energy, which can be achieved by altering the bond lengths or angles between atoms, or more drastically, by fragmenting into smaller pieces. Photoelectron spectroscopy (PES) is a powerful analytical technique that probes the electronic structure of materials by measuring the kinetic energy of electrons ejected upon photon absorption. This technique has become indispensable in various fields, including surface science, materials science, chemistry, and condensed matter physics, providing detailed insights into the electronic states and chemical composition of a wide array of systems.

The foundation of PES lies in the photoelectric effect, first explained by Albert Einstein in 1905 through the use of the new Planck's quantum theory of radiation [1]. Prior to his work, there had been several observations of the photoelectric effect, from the 1887 experiment of H. R. Hertz on the production and detection of electromagnetic waves [2], to the 1902 experiment of Lenard to understand the light intensity dependency of the photoelectric effect [3]. In few words, when photons with sufficient energy strike a material, they can eject electrons from the surface. The kinetic energy of these ejected electrons, measured in PES, provides direct information about the binding energies of electrons in the material [4, 5].

Furthermore, it has to be noted that in Penning ionization PES provides real spectroscopy of the transition state of chemi-ionization reactions [6, 7].

1.2 The Atomic and Molecular Dications and Their Role in Environmental and Astro Chemistry

When two electrons are stripped from a neutral species, a doubly charged cation, known as a dication, is formed. Molecular dications can remain stable against dissociation in the gas phase, even without the stabilizing influence of solvation. The first discovery and identification of a gas-phase molecular dication, CO^{2+}, occurred in the early 20th century during the development of mass spectrometry [8, 9]. Since then, the unique properties of dications have spurred further research, challenging fundamental concepts in chemistry and bonding [10–16]. Dications can be produced through collisions between atoms or molecules and high-energy particles or photons. They have been observed in various high-energy environments, such as comet tails, planetary and satellite ionospheres, the interstellar medium, and near high-energy photon sources [17]. Atomic dications like N^{2+}, O^{2+}, S^{2+}, Ar^{2+}, and Ne^{2+} have been detected in various nebulae, including those in other galaxies, through emission spectroscopy [18, 19]. The presence of dications can influence reactivity in these cold interstellar environments; for instance, they can undergo Coulomb explosion, fragmenting into two monocations with high kinetic energy. This process can create monocations with translational energies of several eV, allowing reaction barriers to be surpassed at low temperatures [20, 21]. Additionally, metal dications, as Mg^{2+}, are believed to facilitate interstellar processes by lowering reaction barriers [22]. Research has shown that both atomic and molecular dications exhibit significant

bimolecular reactivity following collisions with neutral species [23–25]. These collisional processes are expected to be the primary factor limiting the lifetimes of atomic dications in planetary ionospheres [26, 27]. Despite their inherent thermodynamic instability compared to their dissociated charge-separated products, the metastable electronic states of many molecular dications have lifetimes sufficient to allow collisions with other species in planetary environments. For example, the primary loss mechanisms for CO^{2+} and O^{2+} dications in ionospheres are predicted to be bimolecular reactions [28]. The reactive nature of dications, along with their significant presence in ionospheres, suggests that their bimolecular chemistry could play a role in ionospheric chemistry, potentially contributing to the formation of complex molecules. Carbon-carbon coupling reactions have been observed following interactions of aromatic dications with methane [29], ethyne [30], and benzene [31]. Dications from nitrogen-containing compounds, such as pyridine and benzonitrile, have been used in some of these bond-forming reactions, consequently these processes could be relevant to the nitrogen-rich atmosphere of Titan.

By removing two electrons from a neutral species, a formed dication can be an unstable molecule with a variable lifetime that can be long enough to allow the dication to collide with neutral molecules and evolve through a large number of possible processes. However, in general, a molecular dissociation is highly probable: in this case, the dication does not have a lifetime long enough to collide with neutral molecules before its dissociation into fragment ions. In this case, the analysis of emitted electrons and ionic fragments by photoelectron-photoion-photoion coincidence (PEPIPICO) spectroscopy makes it possible to extract fundamental information about the process, such as energy thresholds, kinetic energy released (KERs) and angular distributions of fragment ions [32–35].

A schematic overview of the possible cases that can occur as a result of molecular dication formation in accordance with Eq. (2) below is illustrated in Fig. 1.

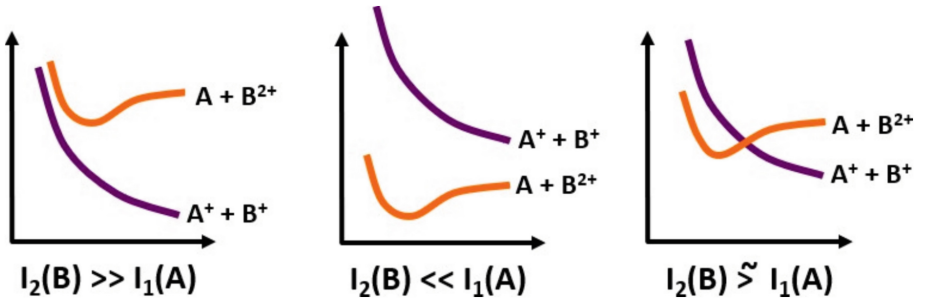

Fig. 1. The scheme of the potential energy curves for the simple case of AB^{2+} diatomic molecular dications. $I_2(B)$ stands for the second ionization potential of the B atom, being the one having the lower electronegativity with respect to A, while $I_1(A)$ is the first ionization potential of the A atom.

Figure 1 shows the scheme of the potential energy curves for the simple case of AB^{2+} molecular dications, in which the first case on the left shows the case of the thermodynamically unstable dications, the center panel the case of stable species that can be detected in gas phase, while the right panel shows molecular dications in a metastable

state, as a result of an avoided crossing of the potential energy curves involved. In Fig. 2, is reported the resulting potential energy curve for this latter case, in which is shown the generation of the two A^+ and B^+ fragment ions that generally carry a high relative kinetic energy release. As mentioned above, this dissociation process takes the name of Coulomb explosion and generates monocations with a translational energy content that, in general, ranges from 1 to 10 eV.

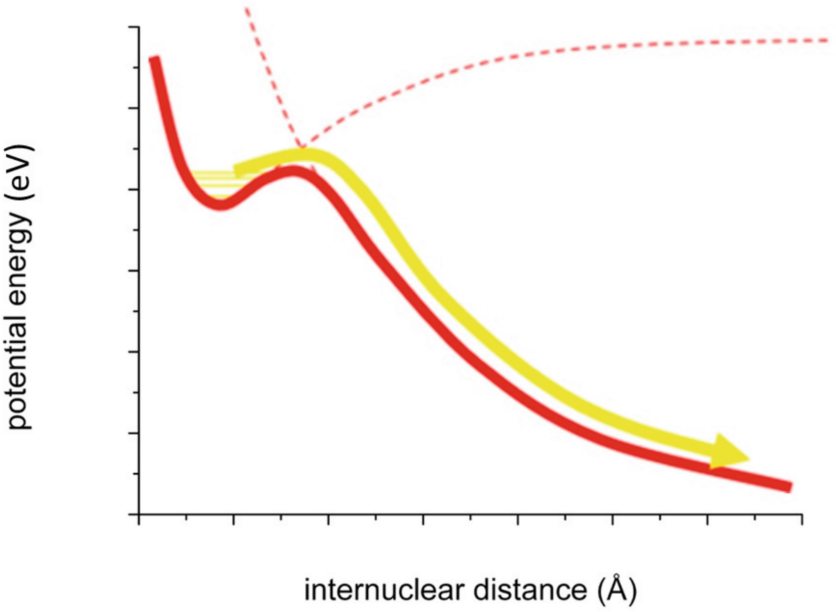

Fig. 2. The resulting potential energy curve, typical for the case of metastable molecular dications AB^{2+} (due to an avoided crossing), generating the two A^+ and B^+ fragment ions (dotted lines) having, in general, a kinetic energy content of several eV.

This kind of process is the responsible for the escape of O^+ ions from Mars' ionosphere, which explains the continuous process of erosion to which this planet's atmosphere is subjected [36–38].

The production and characterization of stable and metastable dications are performed by our research group using PES and PEPIPICO techniques coupled with synchrotron radiation at the ELETTRA Synchrotron Facility of Basovizza (Trieste, Italy).

2 The Elettra Synchrotron Facility

The Elettra Synchrotron Facility, located in Trieste, Italy, is a prominent research center dedicated to the exploration and advancement of synchrotron light applications. Since its inauguration in 1993, Elettra has been at the forefront of scientific research, enabling groundbreaking work across a variety of disciplines, including physics, chemistry, biology, and materials science. Operated by "Elettra - Sincrotrone Trieste S.C.p.A.", this

facility serves as a critical resource for both academic and industrial researchers from around the world. This third-generation storage ring operates in top-up mode in both 2 and 2.4 GeV user energies. Elettra features 28 beamlines that have been specifically optimized to deliver photons across an energy range from a few eV to several keV. It achieves a spectral brightness of up to 10^{19} photons/s/mm^2/mrad^2 with a 0.1% bandwidth. To maintain its competitiveness with the latest synchrotron light sources, Elettra undergoes continuous upgrades and improvements. In particular, photoionization studies of environmentally and astrochemically relevant molecular precursors are performed at both the GasPhase and CiPo beamlines.

2.1 The GasPhase and CiPo Beamlines

The Gas Phase Photoemission (GAPH) beamline at Elettra is uniquely dedicated to studying gaseous systems (see Fig. 3).

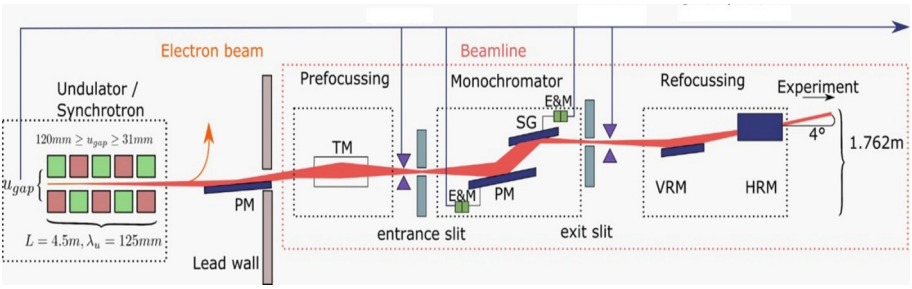

Fig. 3. The Schematic side view of the beamline, reproduced with courtesy of the Elettra Synchrotron Facility (Basovizza, Trieste, Italy).

This beamline offers high-resolution capabilities and provides a high flux across a broad energy range, spanning from 13 to 900 eV. The light beam maintains a stable and nearly circular spot size of approximately 200 μm at the target. An undulator supplies light to the beamline, with energies extending from 13.5 eV to well beyond 900 eV. A "Variable Angle Spherical Grating Monochromator", with fixed slit positions, is used to manage the light's wavelength. The optical design, created by the "Sincrotrone Trieste", incorporates a toroidal prefocusing mirror and two refocusing mirrors-one spherical and the other plane-elliptical. During commissioning, the monochromator not only met but surpassed its design specifications, achieving a resolving power of 60,000 at 48 eV. Even at higher energies, such as 540 eV, it maintains a resolving power above 10,000, and reaches 8,000 at 860 eV, making it the most precise monochromator at Elettra. The inclusion of two refocusing mirrors helps produce a nearly circular beam spot at the sample, with a diameter exceeding 350 μm when using a 20 μm exit slit. This size decreases to under 150 μm as photon energy surpasses 200 eV. The beamline connects to the experimental station through a differential pumping section, ensuring a five-order-of-magnitude pressure difference. This configuration isolates the ultra-high vacuum (UHV) area of the mirror chambers from the higher vacuum region of the experiment. This layout

supports a broad energy range (approximately 13 to 900 eV) and maintains a high energy resolution ($E/\Delta E > 10{,}000$) throughout. The beam delivers a small, nearly circular spot of light (200 μm × 200 μm) with minimal angular divergence (about 3 mrad) at the sample position, located 2.5 m from the last optical component. These design constraints result in an overall monochromator length of about 6 m, featuring two refocusing mirrors. The second mirror has a short exit arm and adjusts the focus to 1.762 m above the floor at a 4°angle. The monochromator also requires entrance and exit slits with adjustable widths ranging from 5 to 200 μm. The monochromator consists of a plane mirror and five spherical gratings to accommodate the extensive energy range. These gratings vary in radius and ruling. The maximum achievable energy resolution with the Variable Angle Spherical Grating Monochromator (VASGM) is limited by the mechanics of the plane mirror and spherical grating movements. However, resolution can be enhanced over short ranges by adjusting the spherical grating to optimize the plane mirror's focus. Moreover, the resolution depends on the exit slit width, which affects the photon flux. More details and schematics can be found in literature and on the official Elettra website [39].

The Circular Polarization (CiPo) beamline at the ELETTRA Synchrotron is notable for its ability to produce synchrotron radiation with variable polarization, ranging from circular to linear, across a wide photon energy spectrum from 11 to 900 eV. At the heart of the CiPo beamline is the Electromagnetic Elliptical Wiggler (EEW), which is engineered to deliver both linearly and circularly polarized light throughout the entire energy range. The EEW can function in both undulator and wiggler modes. A unique aspect of the EEW is its electromagnetic design, which facilitates helicity switching by integrating horizontal and vertical periodic magnets into a single open-side structure. In wiggler mode, the EEW operates with varying horizontal and vertical magnetic field strengths to produce elliptically polarized radiation, offering a continuous emission spectrum from 40 eV to over 1000 eV. It also generates a spectrum of harmonics at the lower end of the photon energy range, below 40 eV. The degree of circular polarization varies with photon energy, starting at 40% at 8.5 eV and reaching 80% at 575 eV. Full circular polarization is achieved when the EEW acts as a pure circular undulator, with equal horizontal and vertical magnetic fields. In undulator mode, the EEW can also produce linearly polarized radiation, with the polarization vector aligned either parallel or perpendicular to the orbit plane. The beamline features two monochromators: a Normal Incidence Monochromator (NIM) for low energies between 5 and 35 eV, and a Spherical Grating Monochromator (SGM) for higher energies. More details and schematics can be found in literature and on the official Elettra website [40].

The used apparatus in our experiments, hosting a PES as well as a PEPICO detector for the characterization of generated molecular dications is the ARPES (Angle Resolved PhotoEmission Spectroscopy)-end station, described in the next subsection.

2.2 The ARPES-End Station

The ARPES-end station used for the experimental measurements on molecular dications is an ion imaging spectroscopy apparatus equipped with a differential pumping system (see Fig. 4). This system allows the use of two interchangeable molecular beam setups: a pyrolytic source and a hypodermic needle. The apparatus enables photoionization studies using a tunable, high- photon flux from a third-generation synchrotron source.

These studies primarily rely on PES and PEPIPICO detectors paired with a time-of-flight (TOF) mass spectrometer, specifically designed to measure the spatial momentum components of ion fragments in double photoionization experiments [40]. In the past, this particular end station has been successfully employed in double photoionization studies of HX molecules (where X = Cl, Br, and I) [14, 41].

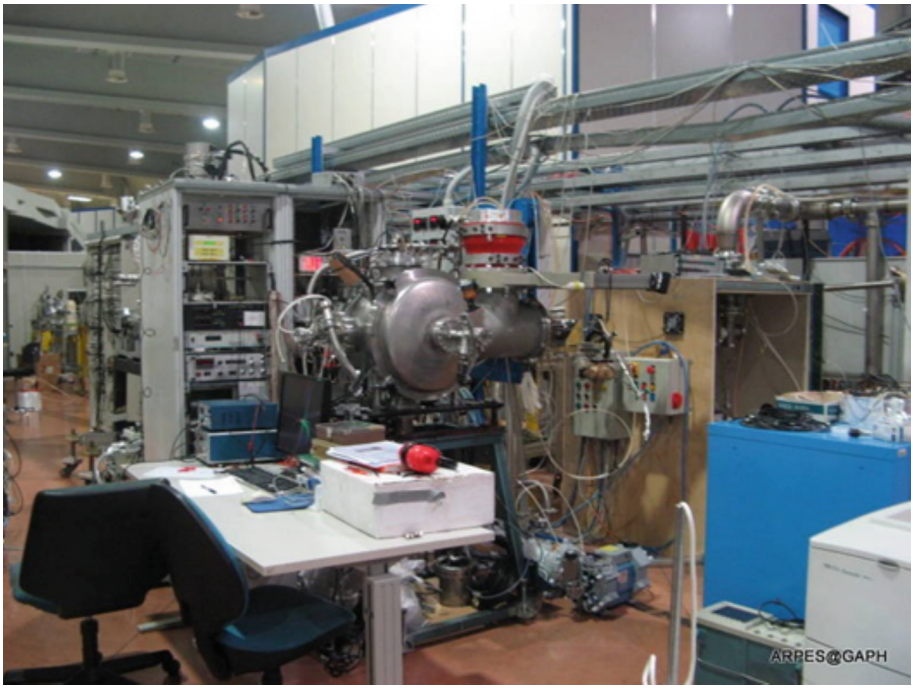

Fig. 4. The ARPES-end station apparatus operating at the GasPhase beamline of Elettra Synchrotron Facility (Trieste, Italy).

The experimental procedure and the relative computational analysis of collected observables are fully described in detail in previous papers [42, 43].

Briefly, a stainless-steel needle was used to introduce the sample as an effusive beam into the chamber. During the experiment, synchrotron radiation within the appropriate energy range passes through a monochromator, which uses a 400 lines/mm spherical grating in first-order diffraction. The slits are adjusted to achieve a photon energy resolution of about 1.5 meV. A magnesium filter is used to eliminate spurious ionization effects caused by photons from higher diffraction orders. The radiation then intersects the beam of the target molecule in the extraction region. Electrons are accelerated towards a micro-channel plate (MCP) detector and serve as triggers for ion time-of-flight measurements. Ions are extracted, accelerated through a TOF spectrometer, and mass-selected. The photon flux interacting with the target beam and the gas pressure are continuously monitored. Ion yields are adjusted for fluctuations in pressure and photon flux whenever

the photon energy changes. Additionally, the gas inlet source uses a mixture of the target molecule and helium to normalize all ion signals at each photon energy to the total ion yield of helium. Ion impacts create electron clouds that are collected by a position-sensitive detector, which comprises 64 strip anodes (32 vertical and 32 horizontal). Each anode is connected to an independent time-to-digital converter (TDC), allowing for the detection of multiple ion fragments and electrons from a single photoionization event. A discriminator is also connected to the 64 detectors. After an event occurs, the TDC sends signals to a Versa Module Eurocard (VME), which transmits the data to an acquisition computer. This computer records the data, specifically logging the x and y positions of each particle hit, meaning that for each ion, two spatial coordinates and one temporal coordinate are documented. The detected ions are categorized into groups of single, double, triple, and higher-order coincidences for each start electron.

3 Synthesis of Isothiocyanic Acid (HNCS)

The isothiocyanic acid (HNCS, see Fig. 5), the simplest isothiocyanate, is the most stable member of the [H,N,C,S] isomer family. Early experimental work assumed that the NCS chain in HNCS was strictly linear. However, ab initio calculations later challenged this notion, leading to a new evaluation of its structural parameters [44].

HNCS was first detected in the interstellar medium in 1979 within the giant molecular cloud Sgr B2, and since then, its presence in both interstellar and terrestrial environments has been well-established [45], prompting extensive studies on neutral and singly charged HNCS. Photolysis at low temperatures led to the observation of its isomers, HSCN and HSNC. In 1970, Eland characterized the spectral bands of the single ionization photoelectron spectrum of HNCS [46]. Over two decades later, Ruscic and Berkowitz determined the appearance energy of singly charged fragments and the H-NCS bond energy. Gronowski's ab initio calculations further confirmed the existence of neutral HNCS and its cation in the interstellar medium [47].

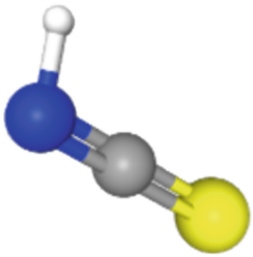

Fig. 5. 3D visualization of the HNCS structure.

The preparation of HNCS has been performed directly in the spectrometer laboratory, due to the high instability of the sample, that tends to autopolymerize in a matter of minutes if not held at a low temperature. The procedure followed was based on the work of John Eland [46], with some modifications in order to optimize time and yield.

The reagents used for the synthesis are potassium thiocyanate (KSCN) and potassium bisulphate ($KHSO_4$), with a 1:1 molar ratio, following the reaction:

$$KHSO_4 + KSCN \rightarrow HSCN + K_2SO_4 \quad (1)$$

The product of the reaction is formally thiocyanic acid, HSCN, which exists as a tautomer with isothiocyanic acid, HNCS, according to the following reaction:

$$HNCS(g) \leftrightarrow HNCS(g) \quad (2)$$

In gaseous phase the isothiocyanic acid tautomer tends to dominate with the compound being about 95% of the total.

The preparation scheme is illustrated in Fig. 6, it consists of a glass test tube designed to be connected to the spectrometer through a KF flange, in which are inserted the reagents, previously finely grounded and put in separate vacuum desiccators over phosphorous pentoxide, P_2O_5, for several days, to remove any trace of water, in which HNCS is soluble.

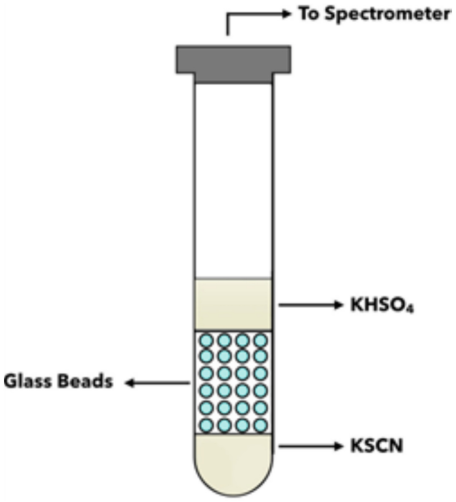

Fig. 6. Scheme of the test tube used in the preparation of gaseous HNCS.

Between the two layers of reagents are placed some glass beads, to maintain the two compounds separated. The test tube has been pumped for 24 h and then immerged in liquid nitrogen (LN_2), to prevent the start of the polymerization reaction at room temperature once the reagents are mixed together. The test tube has then been shaken manually to mix the two reagents and quickly put back in LN_2, this cycle has been repeated several times to assure a complete mixing of the two compounds. The tube has been attached to the gas inlet system in a slush bath composed of a mixture of LN_2 and ethanol, at -80 °C, and pumped again for several minutes; after this cycle, the experimental run has been conducted with the test tube immerged in a slush bath at -10 °C, in order to slow down the inevitable polymerization reaction and to allow the measurement to run for several hours.

4 Synthesis of Carbon Suboxide (C_3O_2)

The carbon suboxide (see Fig. 7) has been detected in ambient air samples and is considered a potential pollutant and precursor to oxidants, but its atmospheric lifetime and behavior remain largely uncertain. It has been synthesized for the first time by Diels and Wolf in 1906 [48]. At room temperature, this gas is lacrimatory, with a pungent odor that can irritate the eyes, nose, and respiratory system. Structurally, C_3O_2 is a quasi-linear cumulene with the formula O = C = C = C = O, featuring a shallow W-shape that easily deforms due to bending vibrations and a weak dipole moment. Although carbon suboxide has some applications in organic synthesis, it also appears as an intermediate in the abiotic degradation of aromatics in soils [49], is released during the incomplete combustion of biofuels and biomass [50], and might exist in extraterrestrial environments [51, 52]. Due to its hydrolysis into malonic acid, which suggested it would not be present in the atmosphere at detectable levels, the chemistry of C_3O_2 in the atmosphere has not been extensively studied yet.

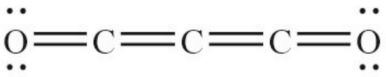

Fig. 7. Lewis structure of C_3O_2.

Carbon suboxide has been synthetized through the dehydration of malonic acid with P_2O_5 [48, 53]. The reaction is set to happen at 145 °C and the major product of it is CO_2, with C_3O_2 and acetic acid (CH_3COOH) being the minor products:

$$2C_3H_4O_4 \rightarrow C_3O_2 + CO_2 + CH_3COOH + 2H_2O \tag{3}$$

The setup consists of a two or three necked flask, connected to a thermometer and to a Liebig condenser, without water reflux active, or to a simple bridge, attached to a receiving flask placed in a dewar filled with liquid nitrogen (see Fig. 8). The entire reaction takes place under vacuum ($\approx 10^{-2}$ mbar).10 to 12 g of malonic acid have been finely grounded and put to dry in a desiccator for a few days, then mixed with 50 g of P_2O_5 and 20 g of roasted sand and added to the main flask, previously cleaned and set under vacuum to remove any trace of moisture. The flask has been placed in a heating mantle with the possibility to control the temperature rising. Despite reaching 145 °C externally, considering the resistance of the glass of the flask the internal temperature has reached a peak of 130 °C. Over the course of two hours, a white solid has condensed into the receiving flask; at the end of the reaction, the receiving flask has been detached from the system, and the product left to thaw under the fume hood, due to the lacrimatory effect that C_3O_2 possess, and transferred when liquid ($C_3O_{2mp} = -110$ °C) in a test tube with a KF junction. The sample has then been purified by being placed in a ethanol/LN_2 bath at −78 °C and pumped for several cycles, in order to remove all the CO_2; regarding acetic acid, very few to no traces have been detected experimentally. In the end, 1 to 1.5 ml of carbon suboxide have been collected, resulting in a yield of about 10%, consistent with the rate reported in literature. Due to its highly unstable nature, every sample has been available for an experimental run for no longer than two days, at room temperature, with the polymerization reaction taking over despite the purification.

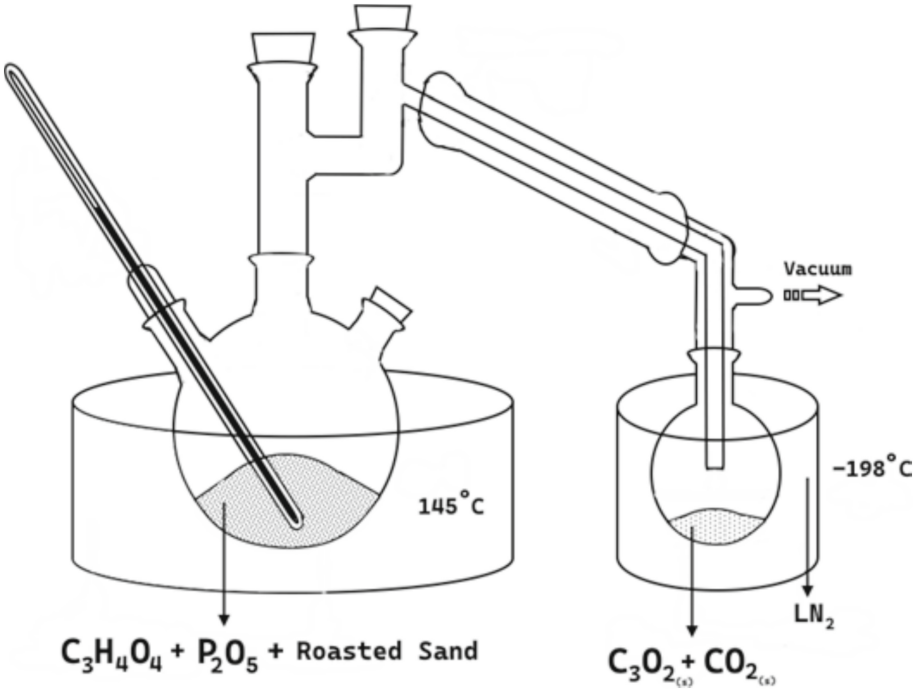

Fig. 8. Scheme of the experimental setup for the synthesis of C_3O_2.

5 Synthesis of Cyanoacetylene (C_3HN)

C_3HN is the simplest cyanopolyne (see Fig. 9).

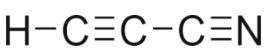

Fig. 9. Lewis structure of C_3HN.

It has been one of the earliest organic molecules identified in the interstellar medium (ISM) [54, 55]. C_3HN and C_5HN have been also found in abundance within solar-type protostars, as evidenced by recent studies [56]. Notably, C_3HN has been identified in comet C/1995 O1 (Hale-Bopp), suggesting that organic molecules like these may contribute to the interstellar organic chemistry legacy passed on to newly formed solar systems. [57]. Cyanoacetylene plays a crucial role in chain elongation processes, reacting with the C_2H radical to produce C_5HN. Conversely, when cyanoacetylene reacts with the CN radical, it leads to a chain termination reaction, forming dicyanoacetylene (C_4N_2). Although dicyanoacetylene and other higher dicyanopolynes have not been detected in the ISM due to their lack of a permanent electric dipole moment, making them undetectable through rotational spectroscopy, they are believed to be prevalent in interstellar and circumstellar clouds, contributing significantly to the total carbon budget [58]. The reaction between CN radicals and cyanoacetylene is also considered the

primary source of C_4N_2, which has been observed in Titan's upper atmosphere, Saturn's largest moon [59–61].

Cyanoacetylene has been synthetized by dehydration of propiolamide (C_3H_3NO) with P_2O_5 at 225 °C [62], following the reaction:

$$C_3H_3NO \rightarrow C_3HN + H_2O \tag{4}$$

The propiolamide has been purchased from Merck. The reaction setup consists in a three- necked round bottom flask connected to a vacuum pump and to a receiver placed in liquid nitrogen, with the whole setup placed under vacuum before the start of the experiment to remove any moisture present (see Fig. 10). 5 g of propiolamide have been mixed with 20 g of P_2O_5 and 20 g of roasted sand, and added to the flask; after that, the temperature has been raised to 225 °C over the course of two hours, and about 3g (60%) of white solid has been collected in the receiving flask and stored under vacuum at −20 °C before using it on the beamline at Elettra. When attached to the spectrometer, the sample has been kept around −30 °C and showed an adequate vapour pressure to perform the experiment for 14 days, with the surplus of the sample that has been put away at −20 °C after the end of the investigation.

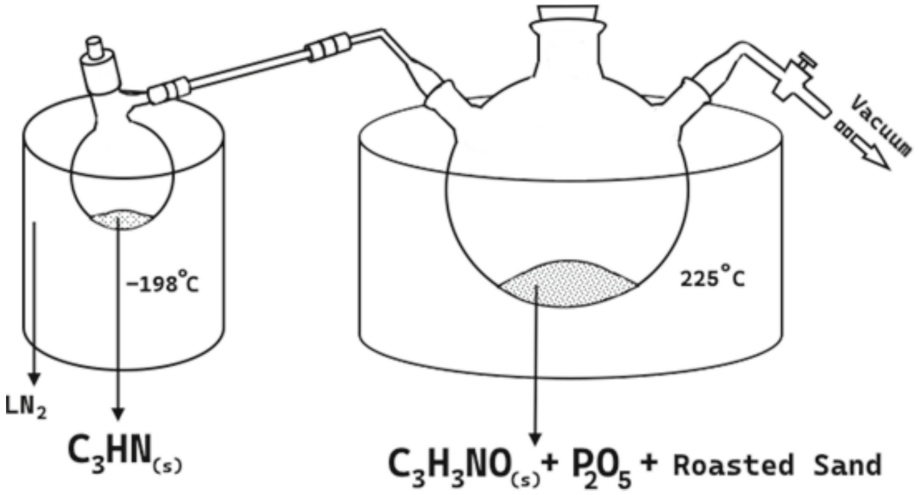

Fig. 10. Scheme of the experimental setup for the synthesis of C_3HN.

Acknowledgments. Dr. Robert Richter, a valued friend and collaborator, died during the preparation of the manuscript. This work and our future efforts are dedicated to him, whose intellectual honesty and genuine love for physics and chemistry continue to inspire our scientific life. This work has been funded by the European Union – NextGenerationEU under the Italian Ministry of University and Research (MUR) National Innovation Ecosystem (grant number ECS00000041) - VITALITY - CUP J97G22000170005. M.P. acknowledges the Italian Space Agency (ASI, DC-VUM-2017–034, Grant no. 2019–3 U.0 Life in Space).

Disclosure of Interests. The authors have no competing interests to declare that are relevant to the content of this article.

References

1. Einstein, A.: Über einen die Erzeugung und Verwandlung des Lichtes betreffenden heuristischen Gesichtspunkt. Ann. Phys. **322**(6), 132–148 (1905)
2. Jenkin, J.G., Riley, J.D., Liesegang, J., Leckey, R.C.G.: The development of x- ray photoelectron spectroscopy (1900–1960): a postscript. J. Electron Spectrosc. Relat. Phenom. **14**(6), 477–485 (1978)
3. Wheaton, B.R.: Philipp Lenard and the photoelectric effect, 1889–1911. Hist. Stud. Phys. Sci. **9**, 299–322 (1978)
4. Hüfner, S.: Photoelectron Spectroscopy: Principles and Applications, 3rd edn. Springer, Berlin, Heidelberg (2003)
5. Oswald, S.: X-ray photoelectron spectroscopy in analysis of surfaces. Encyclopedia of Analytical Chemistry: Applications, Theory and Instrumentation. John Wiley & Sons, Ltd., Hoboken (2006)
6. Brunetti, B.G., Candori, P., Falcinelli, S., et al.: The stereodynamics of the penning ionization of water by metastable neon atoms. J. Chem. Phys. **139**(16), 164305 (2013)
7. Falcinelli, S., Farrar, J.M., Vecchiocattivi, F., Pirani, F.: Quantum-state controlled reaction channels in chemi-ionization processes: radiative (optical−physical) and exchange (oxidative−chemical) mechanisms. Acc. Chem. Res. **53**(10), 2248–2260 (2020)
8. Conrad, R.: The appearance of doubly positively charged molecules in a beam of canal rays. Phys. Z. **31**, 888–892 (1930)
9. Vaughan, A.L.: Mass spectrograph analyses, and critical potentials for the production of ions by electron impact, in nitrogen and carbon monoxide. Phys. Rev. **38**(9), 1687 (1931)
10. Pauling, L.: The normal state of the helium molecule-ions He_2^+ and He_2^{++}. J. Chem. Phys. **1**, 56–59 (1933)
11. Falcinelli, S., Fernandez-Alonso, F., Kalogerakis, K., Zare, R.N.: Mass spectrometric detection of alkaline earth monohalide dications. Mol. Phys. **88**(3), 663–672 (1996)
12. Brunetti, B., Candori, P., De Andres, J., et al.: Dissociative ionization of methyl chloride and methyl bromide by collision with metastable neon atoms. J. Phys. Chem. A **101**(41), 7505–7512 (1997)
13. Alagia, M., Brunetti, B.G., Candori, P., et al.: Threshold-photoelectron-spectroscopy-coincidence study of the double photoionization of HBr. J. Chem. Phys. **120**(15), 6980–6984 (2004)
14. Alagia, M., Brunetti, B.G., Candori, P., et al.: Low-lying electronic states of HBr^2+. J. Chem. Phys. **120**(15), 6985–6991 (2004)
15. Bartocci, A., Belpassi, L., Cappelletti, D., et al.: Catching the role of anisotropic electronic distribution and charge transfer in halogen bonded complexes of noble gases. J. Chem. Phys. **142**(18), 184304 (2015)
16. Pirani, F., Cappelletti, D., Falcinelli, S., et al.: Selective emergence of halogen bond in ground and excited states of noble-gas—chlorine systems. Angew. Chem. **58**(13), 4195–4199 (2019)
17. Falcinelli, S., Rosi, M.: Production and characterization of molecular dications: experimental and theoretical efforts. Molecules **25**, 4157 (2020)
18. Wilkes, B.J., Ferland, G.J., Hanes, D., Truran, J.W.: On nitrogen abundances of planetary nebulae. MNRAS **197**(1), 1–6 (1981)
19. Greenberg, L.T., Dyal, P., Geballe, T.R.: Detection of forbidden S III fine-structure emission in ionized nebulae. Astrophys. J. **213**, L71–L74 (1977)

20. Böhme, D.K.: Multiply-charged ions and interstellar chemistry. Phys. Chem. Chem. Phys. **13**(41), 18253–18263 (2011)
21. Alagia, M., Candori, P., Falcinelli, S., et al.: Anisotropy of the angular distribution of fragment ions in dissociative double photoionization of N_2O molecules in the 30–50 eV energy range. J. Chem. Phys. **126**(20), 201101 (2007)
22. Thripati, S., Ramabhadran, R.O.: Pathways for the formation of formamide, a prebiotic biomonomer: metal-ions in interstellar gas-phase chemistry. J. Phys. Chem. A **125**(16), 3457–3472 (2021)
23. Tosi, P., Correale, R., Lu, W., et al.: Production of the molecular dication ArN^{2+} in the reaction Ar^{2+}+N_2. Phys. Rev. Lett. **82**(2), 450–452 (1999)
24. Price, S.D., Fletcher, J.D., Gossan, F.E., Parkes, M.A.: Bimolecular reactions of the dications and trications of atoms and small molecules in the gas-phase. Int. Rev. Phys. Chem. **36**(1), 145–183 (2017)
25. Ascenzi, D., Aysina, J., Zins, E.-L., et al.: Double ionization of cycloheptatriene and the reactions of the resulting $C_7H_n{}^{2+}$ dications (n = 6, 8) with xenon. Phys. Chem. Chem. Phys. **13**(41), 18330–18338 (2011)
26. Thissen, R., Witasse, O., Dutuit, O., et al.: Doubly-charged ions in the planetary ionospheres: a review. Phys. Chem. Chem. Phys. **13**(41), 18264–18287 (2011)
27. Falcinelli, S., Pirani, F., Alagia, M., et al.: Molecular dications in planetary atmospheric escape. Atmosphere **7**(9), 112 (2016)
28. Gu, H., Cui, J., Niu, D.D., et al.: Observation of $CO_2{}^{++}$ dication in the dayside martian upper atmosphere. Earth Planet. Phys. **4**(4), 396–402 (2020)
29. Ricketts, C.L., Schröder, D., Alcaraz, C., Jana Roithová, J.: Growth of larger hydrocarbons in the ionosphere of titan. Chem. A Eur. J. **14**(16), 4779–4783 (2008)
30. Roithová, J. and Schröder, D.: On a possible growth mechanism for poly- cyclic aromatic hydrocarbon dications: $C_7H_6{}^{2+} + C_2H_2$. Chem. A Eur. J. **13**(10), 2893–2902 (2007)
31. Roithová, J., Schröder, D.: Bond-formation versus electron transfer: C-coupling reactions of hydrocarbon dications with benzene. Phys. Chem. Chem. Phys. J. **9**(6), 731–738 (2007)
32. Alagia, M., Boustimi, M., Brunetti, B.G., et al.: Mass spectrometric study of double photoionization of HBr molecules. J. Chem. Phys. **117**(3), 1098–1102 (2002)
33. Price, S.D.: Coincidence studies of the bond-forming reactivity and reaction dynamics of molecular dications. Int. J. Mass Spectrom. **260**(1), 1–19 (2007)
34. Falcinelli, S., Rosi, M., Candori, P., et al.: Kinetic energy release in molecular dications fragmentation after VUV and EUV ionization and escape from planetary atmospheres. Planet. Space Sci. **99**, 149–157 (2014)
35. Falcinelli, S., Vecchiocattivi, F., Pirani, F., et al.: The fragmentation dynamics of simple organic molecules of astrochemical interest interacting with VUV photons. ACS Earth Space Chem. **3**, 1862–1872 (2019)
36. Witasse, O., Dutuit, O., Lilensten, J., et al.: Prediction of a $CO_2{}^{2+}$ layer in the atmosphere of Mars. Geophys. Res. Lett. **30**, 1360 (2003)
37. Slattery, A.E., Field, T.A., Ahmad, M., et al.: Spectroscopy and metastability of $CO_2{}^{2+}$ molecular ions. J. Chem. Phys. **122**, 084317 (2005)
38. Falcinelli, S., Pirani, F., Alagia, M., et al.: The escape of O^+ ions from the atmosphere: an explanation of the observed ion density profiles on Mars. Chem. Phys. Lett. **666**, 1–6 (2016)
39. Blyth, R.R., Delaunay, R., Zitnik, M., et al.: The high resolution gas phase photoemission beamline. Elettra. J. Electr. Spectr. Rel. Phenom. **101**, 959–964 (1999)
40. Lavollée, M.: A new detector for measuring three-dimensional momenta of charged particles in coincidence. Rev. Sci. Instrum. **70**(7), 2968–2974 (1999)
41. Alagia, M., Brunetti, B.G., Candori, P., et al.: The double photoionization of hydrogen iodide molecules. J. Chem. Phys. **124**(20), 204318 (2006)

42. Falcinelli, S., Rosi M., Candori, P., et al.: Modeling the intermolecular interactions and characterization of the dynamics of collisional autoionization processes. In: Murgante, B., et al. (eds.) ICCSA 2013, LNCS, vol. 7971, pp. 69–83. Springer, Heidelberg (2013)
43. Parriani, M., Giustini, A., Alagia, M., et al.: Data analysis of molecular dications fragmentation processes by double photoionization with synchrotron radiation. In: Gervasi, O., et al. (eds.) ICCSA 2024, LNCS, vol. 14818, pp. 55–70. Springer, Heidelberg (2024)
44. Yamada, K., Winnewisser, M., Winnewisser, G., et al.: Ground state spectroscopic constants of $H^{15}NCS$, $HN^{13}CS$, and $HNC^{34}S$, and the molecular structure of isothiocyanic acid. J. Mol. Spectr. **79**(2), 295–313 (1980)
45. Krupa, J., Kosendiak, I., Wierzejewska, M.: New data on photochemistry of the interstellar molecule: HNCS. identification of the S-HCN complex. Phys. Chem. Chem. Phys. **17**(34), 22431–22437 (2015)
46. Eland, J.H.D.: A discussion on photoelectron spectroscopy-the photo- electron spectra of isocyanic acid and related compounds. Philos. Trans. R. Soc. Lond. Ser. A Math. Phys. Sci. **268**(1184), 87–96 (1970)
47. Ruscic, B., Berkowitz, J.: The H-NCS bond energy, ΔH^o(HNCS), ΔH^o(NCS), and IP (NCS) from photoionization mass spectrometric studies of HNCS, NCS, and $(NCS)_2$. J. Chem. Phys. **101**(9), 7975–7989 (1994)
48. Diels, O., Lalin, L.: Über das kohlensuboxyd. Ber. Dtsch. Chem. Ges. **41**(3), 3426–3434 (1908)
49. Huber, S.G., Kilian, G., Schöler, H.F.: Carbon suboxide, a highly reactive intermediate from the abiotic degradation of aromatic compounds in soil. Environ. Sci. Technol. **41**(22), 7802–7806 (2007)
50. Roblee Jr, L.H.S., Agnew, J.T., Wark, K., Jr.: Evidence for carbon suboxide, C_3O_2, as an intermediate product in the cool flame oxidation products of diethyl ether. Combust. Flame **5**, 65–70 (1961)
51. Bennett, C.J., Jamieson, C.S., Kaiser, R.I.: Mechanistic studies on the decomposition of carbon suboxide in a cometary ice analog. Planet. Space Sci. **56**(9), 1181–1189 (2008)
52. Lasne, J., Noblet, A., Szopa, C., et al.: Oxidants at the surface of mars: a review in light of recent exploration results. Astrobiology **16**(12), 977–996 (2016)
53. Long, D.A., Murfin, F.S., and Williams, R.L.: The Raman and infra-red spectra of carbon suboxide. Proc. R. Soc. Lond. Ser. A. Math. Phys. Sci., **223**(1153), 251–266 (1954)
54. Turner, B.E.: Detection of interstellar cyanoacetylene. Astrophys. J. **163**, L35 (1971)
55. Cabezas, C., Agúndez, M., Endo, Y., et al.: Discovery of the interstellar cyanoacetylene radical cation HC_3N^+. Astron. Astrophys. **687**, L22 (2024)
56. Jaber, A., Edhari, A.L., Ceccarelli, C., et al.: History of the solar-type protostar IRAS 16293–2422 as told by the cyanopolyynes. Astron. Astrophys. **597**, A40 (2017)
57. Mumma, M.J., Charnley, S.B.: The chemical composition of comets - emerging taxonomies and natal heritage. Annu. Rev. Astron. Astrophys. **49**(1), 471–524 (2011)
58. Petrie, S., Millar, T.J., Markwick, A.J.: NCCN in TMC-1 and IRC+ 10216. MNRAS **341**(2), 609–616 (2003)
59. Petrie, S. and Osamura, Y.: NCCN and NCCCCN formation in Titan's atmosphere: 2. HNC as a viable precursor. J. Phys. Chem. A **108**(16), 3623–3631 (2004)
60. Mancini, L., Rosi, M., Skouteris, D., Vanuzzo, G., et al.: A computational characterization of the reaction mechanisms for the reactions N (^{2}D) + CH_3CN and HC_3N and implications for the nitrogen-rich organic chemistry of Titan. Comput. Theor. Chem. **1229**, 114341 (2023)
61. Liang, P., Aragão, E., Pannacci, G., et al.: Reactions O (^{3}P, ^{1}D) + HCCCN ($X^1\sum^+$) (cyanoacetylene): crossed-beam and theoretical studies and implications for the chemistry of extraterrestrial environments. J. Phys. Chem. A **127**(3), 685–703 (2023)
62. Miller, F.A., Lemmon, D.H.: The infrared and Raman spectra of di- cyanodiacetylene, NCCCCCCN. Spectrochim. Acta A: Mol. Biomol. Spectrosc. **23**(5), 1415–1423 (1967)